DOE/NASA/51040-58
NASA TM-86875

Initial Testing of a Variable-Stroke Stirling Engine

Lanny G. Thieme
National Aeronautics and Space Administration
Lewis Research Center

February 1985

Prepared for
U.S. DEPARTMENT OF ENERGY
Conservation and Renewable Energy
Office of Vehicle and Engine R&D

Printed in the United States of America

Available from
National Technical Information Service
U.S. Department of Commerce
5285 Port Royal Road
Springfield, VA 22161

NTIS price codes[1]
Printed copy: A02
Microfiche copy: A01

[1]Codes are used for pricing all publications. The code is determined by the number of pages in the publication. Information pertaining to the pricing codes can be found in the current issues of the following publications, which are generally available in most libraries: *Energy Research Abstracts (ERA); Government Reports Announcements* and Index (*GRA* and I); *Scientific and Technical Abstract Reports (STAR);* and publication, NTIS-PR-360 available from NTIS at the above address.

DOE/NASA/51040-58
NASA TM-86875

Initial Testing of a Variable-Stroke Stirling Engine

Lanny G. Thieme
National Aeronautics and Space Administration
Lewis Research Center
Cleveland, Ohio 44135

February 1985

Work performed for
U.S. DEPARTMENT OF ENERGY
Conservation and Renewable Energy
Office of Vehicle and Engine R&D
Washington, D.C. 20545
Under Interagency Agreement DE-AI01-77CS51040

INITIAL TESTING OF A VARIABLE-STROKE STIRLING ENGINE

Lanny G. Thieme
National Aeronautics and Space Administration
Lewis Research Center
Cleveland, Ohio 44135

SUMMARY

As part of the Department of Energy's Stirling Engine Highway Vehicle Systems Program, NASA Lewis is investigating the use of variable stroke as an alternative to the complex mean-pressure control system for controlling the power output of an automotive Stirling engine. For this purpose the Advenco (Advanced Engine Concept) Stirling engine has been purchased from Philips Research Laboratories of the Netherlands.

The Advenco is a four-cylinder, double-acting engine designed for a maximum engine output of 44 kW with hydrogen working fluid at a design mean compression-space pressure of 10 MPa. Variable-stroke operation is achieved with a variable-angle swash-plate drive system. The stroke can be varied from 10 mm at a 5° swash-plate angle to 48.5 mm at a 22° swash-plate angle.

Steady-state performance tests were run over a limited range of stroke, mean compression-space pressure, and engine speed with helium working fluid. For constant pressure and speed, the engine power output varied approximately with the square of the stroke. Considering all testing to date (with helium working fluid) the maximum brake power and brake gross thermal efficiency obtained were 5.10 kW and 19.3 percent, respectively. These values were recorded for a run at 5 MPa mean compression-space pressure and a 35 mm stroke.

While attempting to continue an upward progression of pressure and stroke, a major drive system failure occurred. A sleeve on one end of a crosshead seized in its bore, causing extensive damage to the drive system. Repairs and corrective measures were completed before resuming testing. These included properly aligning the crosshead bores in the two separate crankcase sections, plating the crossheads rather than sleeving, and adding pressurized lubrication to the crosshead bores of the rear crankcase.

Finally, computer simulation predictions were made comparing steady-state performance at part loads obtained tow ways: (1) by varying the stroke at maximum pressure (variable-stroke control) and (2) by varying the pressure at maximum stroke (mean-pressure control). These predictions indicated a part-load efficiency gain for variable stroke control that increased with increasing engine speed and decreasing power level. These efficiency gains are primarily due to lower flow losses through the heat exchangers and to reduced heat losses that tend to decrease with reduced stroke and pressure ratio (such as shuttle losses).

INTRODUCTION

This work was done in support of the U.S. Department of Energy (DOE) Stirling Engine Highway Vehicle Systems Program. The NASA Lewis Research Center, through interagency agreement DEAI01-77CS51040 with DOE, is responsible

for management of the project under the program direction of the DOE Office of Conservation, Division of Vehicle and Energy R&D.

The power output of most kinematic Stirling engines is varied by changing the mean pressure level of the working fluid. For automotive applications a complex mean-pressure control system is required with attendant reliability and maintenance problems. Also, with this control system the many connections to the working space add more potential leakage paths for the working fluid. These possible problems have raised interest in investigating alternatives to the mean-pressure control system for controlling the power output of a Stirling engine.

This interest led to the purchase of the Advenco (Advanced Engine Concept) Stirling engine from Philips Research Laboratories of the Netherlands. The engine is a four-cylinder, double-acting engine designed for a maximum engine output of about 44 kW with hydrogen working fluid. The major difference between this and current kinematic Stirling engines is the use of variable stroke as a method of power control. The stroke is varied with a variable-angle swash-plate drive system.

Philips tried two other advanced concepts in their original version of this engine. One was using ceramic liners in the regenerator housings and cylinders of the heater head to reduce the amount of expensive heat-resistant materials needed in the engine. The use of liners would permit the use of an inexpensive steel for the housing. However, problems were encountered in installing the liners into the heater head. Thus, the engine as delivered to Lewis has a standard all-metal heater head without the ceramic liners. The other new idea was to enclose the rollsock shaft seal in a cartridge assembly to allow for easier replacement. This assembly is used on the engine as purchased by Lewis.

The objectives of the Advenco testing at Lewis are as follows:

(1) To evaluate the benefits of variable-stroke control (relative to mean-pressure control) in terms of increased engine efficiency, reduced control-system complexity, and reduced working-fluid leakage

(2) To evaluate the variable-angle swash-plate drive as a system for obtaining variable stroke

(3) To investigate any functional problems of operation over a range of strokes

The Advenco engine has been installed in a test cell at Lewis Research Center. Planned testing includes a steady-state evaluation over a range of strokes and pressures to allow comparison of engine performance obtained (1) by varying pressure at constant stroke and (2) by varying stroke at constant pressure. Following the steady-state tests a simplified transient evaluation of the power control system will be made.

Initial testing concentrated on solving a number of problems involving the power control system, the sealing areas in the cooling block, the rollsock cartridge assembly, and the seals on the rotating preheater core. With everything functioning properly, steady-state tests with helium working fluid were begun. Thirty-six data points were taken before a major failure occurred in

the crankcase. A sleeve on one end of a crosshead seized in its bore causing extensive damage to the drive system. Repairs and corrective measures were made before testing was resumed.

This report describes the Advenco Stirling engine and its test setup at Lewis. Results of the initial tests are presented as well as a description of the drive system failure and subsequent engine modifications. Several computer simulation predictions are shown comparing steady-state performance obtained by varying stroke with that obtained by varying pressure.

APPARATUS AND PROCEDURE

Description of Advenco Stirling Engine

The Advenco engine is a four-cylinder, double-acting Stirling engine designed for a maximum output of about 44 kW with hydrogen working fluid. The Advenco was built by Philips Research Labs of the Netherlands. The engine burns natural gas as a fuel and uses rollsock shaft seals. The drive system is a variable-angle swash-plate drive which varies piston stroke to control engine power output. The stroke can be varied from 10 mm at a 5° swash-plate angle to 48.5 mm at a 22° swash-plate angle. The design mean-pressure level is 10 MPa. The efficiency was maximized at a part-power condition corresponding to a 14° swash-plate angle and a 4500 rpm engine speed.

Figure 1 presents photographs of the Advenco engine in its test facility at Lewis, and figure 2 shows a cross-section of the engine. The Advenco engine is further described as originally manufactured by Philips Research Laboratories in reference 1.

Burner-preheater system. - Natural gas enters the vortex gas burner (fig. 3) through the two long tubes entering the top of the burner and is injected into the mixing chamber through small holes in the vertical distribution struts. Air for combustion enters between the struts as well as through the burner cone. Two spark plugs are used with the spark jumping between them.

The preheater uses a rotating ceramic core similar to that used in the Ford-Philips 4-215 Stirling engine (described in ref. 2). The core, driven by a separate electric motor, rotates at 10 rpm. It is sealed on its inner and outer diameters on both the hot and cold sides with flat seals backed by diaphragms and support structures.

Heater head and cooling block. - Figure 4 shows a photograph of the heater head and regenerators. The heater head is a one-piece unit and consists of the heater tubes, regenerator housings, hot ends of the cylinders, and connecting manifolds. Insulation is packed in the area around the regenerator housings, cylinder, and manifolds. There are a total of 60 Multimet N-155 heater tubes, 15 per Stirling cycle. Four of the tubes contain thermocouples, which measure working fluid temperature. Four more thermocouples, spaced circumferentially around the heater cage, measure heater-tube outside metal temperature on the flame side of the first row of heater tubes.

The regenerator (fig. 5), consisting of a sintered stack of fine-mesh stainless-steel wire screens, is threaded into the baseplate of the heater head. The cooler (also fig. 5) consists of a bundle of stainless steel

(AISI 321) tubes. Each Stirling cycle has one cooler and one regenerator.

The cast aluminum cooling block (fig. 6) contains the coolers, the cold ends of the cylinders, cooling water passages for the coolers and cylinders, and the connecting gas passages between the coolers and the cylinders. Each cycle has two check valves installed in the cooling block for working-gas charging and venting. A manifold ties together the four check valves for charging; another manifold connects the four check valves for venting.

The tube shown in the upper left of figure 6 ties the two manifolds together. A capillary is installed in this tube. During engine operation, the manifold for pressurization stores the minimum cycle pressure, and the manifold for venting stores the maximum cycle pressure. If the engine stroke is reduced, the minimum cycle pressure increases, and the maximum cycle pressure decreases. Without the capillary path, the pressures in the manifolds cannot adjust as the check valves will not open. By allowing a small leakage flow between the manifolds, the capillary permits the proper pressure levels to be reestablished in the manifolds. A short-circuit valve (not shown) is also installed between the two manifolds as part of the safety shutdown system.

Pistons and rollsock shaft seals. - A piston and rollsock cartridge and seal are shown in figure 7. The piston is made with a separate dome and base. The Inconel X750 dome is threaded onto the piston base. The base is clamped to the piston rod by tightening a tapered steel cone. Each piston is sealed with two sets of piston rings. Each set has an inner metal ring and an outer ring of Rulon LD. The space inside the dome is connected with the space between the two sets of rings.

One end of the polyurethane rollsock seal is clamped to the stationary housing of the cartridge; the other end is clamped between two tubes inside the cartridge. These tubes slide over the piston rod on installation of the cartridge and then reciprocate with the rod. They are sealed against the rod with an O-ring. This arrangement allows careful assembly of the rollsock seal inside the cartridge. The cartridge assembly can, then, easily be installed in the engine.

The pressure differential across the rollsock seal must be held constant at about 5 atm. A cap seal above the rollsock isolates it from engine cycle pressure variations. The minimum cycle pressure from the proper manifold is fed to the area above the rollsocks to guarantee that minimum cycle pressure is on the gas side of the rollsock. The back side is supported by oil pressure at a value of 5 atm below the minimum cycle pressure. The oil backup supply system and the pressure regulator to control the pressure differential are discussed in the Test Setup section.

Drive system. - Figure 7 also shows a crosshead and pair of sliders which serve as the attachment between the reciprocating piston rod and the rotating swash plate. The sliders, made by slicing ball bearings, ride on both sides of the swash plate. Each slider rides between the swash-plate surface and a retainer cup. The retainer cups can be seen in figure 7 installed in the crosshead. The one retainer cup serves as a bolt to attach the piston rod to the crosshead.

The crossheads are made of a high-strength aluminum with steel sleeves fitted on each end. Each end of the crosshead runs in a bore in a separate

section of the crankcase (see fig. 2). These two sections are aluminum castings. The bridge of the crosshead rides in a slot in the rear casting.

Oil must be supplied to both sides of the sliders. An oil film is provided on the swash-plate surface by a feed through the main shaft. To lubricate the back side of the slider, oil is fed to the bridge of the crosshead. Passageways in the crosshead and retainer cup carry this oil to the back of the slider.

The variable-angle swash-plate assembly is shown in figure 8. The swash plate rotates with the main shaft. Its surface is made slightly convex, which maintains line contact with the sliders. A balance ring is attached around the outside of the swash plate. The bridge of the crosshead must be deep enough to accommodate the swash plate and the balance ring.

To change the angle of the swash plate, hydraulic fluid is ported through concentric channels in the main shaft to a vane-type rotary actuary (fig. 8) mounted behind the swash plate. The hydraulic pressure forces the actuator to rotate relative to the main shaft. This rotation is transmitted by gears to the swash plate. The swash plate's rotation around a tilted section of the main shaft causes the swash-plate angle to change. The control system for adjusting the swash-plate angle is described in the Test Setup section. Further explanation of a variable-angle swash-plate drive system can be found in reference 3.

Test Setup

Schematic diagrams of the Advenco engine test setup are given in figures 9 and 10. Figure 9 shows the oil systems for power control, lubrication, and rollsock support as well as the helium (working gas) pressurization system. Figure 10 shows the cooling water system, air-fuel system for combustion, and the dynamometer for engine load.

Oil systems-power control, lubrication, and rollsock support. - A single reservoir supplies the oil for both the lubrication and rollsock support systems. A separate oil reservoir supplies the oil for the swash-plate-angle actuator in the power control system. An automatic transmission fluid is used in all three oil systems; the oil was chosen in part because of its compatibility with the rollsock seal.

In the engine lubrication system two internal gear pumps, one a pressure pump and the other a suction pump, are chain-driven by the engine to provide lubrication. A third pump in the facility provides oil to the internal engine pressure pump which pumps the oil to the crossheads and retainers and to the swash-plate surface. The suction pump removes oil from the engine crankcase and pumps it back to the reservoir. An oil-to-water heat exchanger is used to maintain the inlet oil temperature at the desired level. Measurements in the oil lubrication system include oil flow, inlet temperature, and temperature rise across the engine. These measurements are used in energy balance calculations.

A separate pump delivers oil to support the backside of the rollsock. As discussed in the engine description, the pressure differential across the rollsock must be controlled to about 5 atm. The oil is pumped to the area

below each rollsock. A line connects this area to the rollsock backup pressure regulator, where excess oil is returned to the reservoir. Seals separate the rollsock oil from the lubrication oil. The pressure regulator equalizes forces on a piston such that $P_{working\ fluid} = P_{oil}$ + spring force. The spring force can be adjusted to give the desired pressure differential. A line connects the oil and working fluid sides of the regulator to provide working fluid to both sides of the rollsock (with the proper pressure differential) if oil pressure is lost; this line normally remains closed.

For the power control system, a high-pressure pump provides oil from a separate reservoir to the hydraulic servovalve. The pressure can be set to values up to 15 MPa to give the desired power response. Engine piston position is measured with a linear variable differential transformer (LVDT) attached to the rear of one of the crossheads. The LVDT output is converted to a voltage signal proportional to the engine stroke. A closed-loop controller then compares this signal with the desired stroke setting and adjusts the hydraulic servovalve to provide oil pressure to the rotary actuator mounted on the main shaft. The rotary actuator changes the swash-plate angle to achieve the desired stroke.

Helium pressurization system. - The helium pressurization system, shown in figure 9, can pressurize or vent the engine through the appropriate check valves in the cooling block. Pressure transducers measure the minimum cycle pressure stored in the pressurization manifold and the maximum cycle pressure stored in the vent manifold. The two manifolds are tied together by the capillary tube (discussed in the engine description) and by a short-circuit valve for safety shutdown. The schematic of figure 9 also shows that the pressurization manifold is tied to the area above the rollsock seals.

Cooling-water system. - The cooling-water system is shown in figure 10. A closed-loop controller mixes water passed through a heat exchanger with water bypassing the heat exchanger to control the inlet temperature to the engine. The flow rate can be varied independently by a throttling flow control valve. Water flow rate, inlet temperature and pressure, and temperature rise across the engine are measured.

Air-fuel system for combustion. - The air blower for the air-fuel system is located downstream of the combustion chamber; thus, the combustion chamber is maintained at a slight negative pressure relative to atmospheric pressure. A variable-speed drive and controller vary the amount of combustion airflow to give the desired heater temperature. One of the four thermocouples measuring heater-tube gas temperature is used to control the heater temperature. The temperature can be controlled automatically or manually. Combustor inlet air flow rate and temperature as well as combustor exhaust pressure and temperature are measured. The natural gas fuel is controlled by a mechanical controller which varies the fuel flow to maintain a relatively constant air-fuel ratio. The controller maintains 40 percent excess air except at low fuel flows, where greater amounts of excess air are provided. Natural gas mass flow rate, pressure, and temperature are measured.

Dynamometer. - A direct-current dynamometer with a low-friction, oil-floated, cradle bearing system absorbs the engine power output. The dynamometer is capable of 180 kW absorbing and 168 kW motoring. Torque is measured with a system of two load cells - one for the higher-range torques and one to provide accuracy in the lower range (<100 N-m). The computer-controlled

dynamometer can be programmed to follow a road load in transient testing modes. Engine speed is measured in two places using magnetic pickups on both sides of the coupling to the dynamometer. Engine stroke is determined electronically from the LVDT signal; the LVDT measures piston position and is attached to the rear of one of the crossheads.

Data acquisition system. - A minicomputer-based digital data recording and display system is used in Advenco testing. The system is intended primarily for steady-state data recording. Its high sampling rate (~5000 samples/sec) allows the acquisition of multiple scans for data averaging of each data point recorded. Ten scans are normally recorded over a 20-sec period for each steady-state data point. The scans are averaged, and statistical information is calculated to determine the variation in each parameter.

The data system has many on-line features and capabilities. It can display data in millivolts or in engineering units on digital panel meters (DPM) or on preprogrammed cathode ray tubes (CRT). It can perform and display on-line calculations on the continually updated DPM's or CRT's and produce hard-copy printouts of the CRT displays on a local printer. It can limit check measured and calculated values and automatically initiate a warning or relay contact closure should a limit be exceeded.

The data system also contains a "history file" feature which freezes, either manually or automatically, the minicomputer's recent memory of acquired data (recorded at ~2 sec intervals). This feature provides a powerful tool for analyzing engine failures or for examining relatively slow transients. Further information on the data system can be obtained from reference 4.

Test Procedure

Before each engine start, a static pressure check was made. The engine was pressurized with helium to 3 MPa and then isolated from the helium bottle. The pressure decay was recorded over a 10- to 15-min period. This allowed comparison of leakage conditions before each day's testing.

After engine start, warmup conditions were established at a 5-MPa mean compression-space pressure, 27-mm engine stroke, 2000-rpm engine speed, 625 °C average heater-tube gas temperature, and 50 °C cooling-water inlet temperature. These conditions were maintained for at least 30 min before taking any performance data to allow the engine to reach operating temperatures. Repeating this procedure on each engine startup permitted verification of proper engine operation.

As stated in the Test Setup section, one of the four thermocouples measuring heater-tube gas temperature was used to control the heater temperature. However, it was desired to control the average of all four heater-tube gas temperatures. Thus, a readout of this average temperature was monitored, and the heater temperature control adjusted manually to give the desired temperature. For these tests the average heater-tube gas temperature was controlled to 625 °C, and the cooling-water inlet temperature to 50 °C. The cooling-water flow rate was set at about 0.9 l/sec.

All tests were run with helium working fluid. For each mean-pressure level, a series of runs were made at different engine strokes. For each engine

stroke, the engine speed was varied over the range of 1500 to 3500 rpm in 500 rpm increments. The procedure followed was to start at the lower values of mean compression-space pressure and engine stroke and then progressively increase these parameters.

RESULTS AND DISCUSSION

Test Results

Preliminary testing identified various engine problems in the stroke control system, the gas sealing surfaces of the cooling block, the rollsock assemblies, and the seals on the preheater core.

The stroke control system difficulty was caused by a displacement of one of the concentric tubes that provide hydraulic oil to the rotary actuator. Because of a resulting leak path, no pressure difference could be established in the actuator to vary the swash-plate angle. After the tube was properly aligned no further problems were encountered with the stroke control system.

The O-ring sealing surfaces between the coolers and the cooling block were pitted and scratched. These pits and scratches were removed to provide an adequate sealing surface. Also, the O-ring sealing surfaces below the cylinder liners that seal the upper part of the rollsock cartridges were gouged. The gouges were removed, and the surfaces nickel-plated to give a smooth finish and to restore the surface to the proper diameter.

The rollsock failure occurred when one of the two tubes holding the reciprocating end of the rollsock to the piston rod cracked, allowing leakage past the rollsock. Further problems have been prevented by modifying the rollsock cartridge installation procedure. The tube was redesigned to relieve the stresses at the failure point.

The problem with seals on the preheater core was solved by installing a new preheater housing (with redesigned supports for the core and cold-side seal) and a redesigned support piece for the hot-side seal.

The steady-state performance testing was then begun with helium as the working fluid. The average heater tube gas temperature was controlled to 625 °C. Water inlet temperature was controlled to 50 °C. For each mean pressure level, a series of runs was made at different engine strokes; for each engine stroke, data points were taken over a range of engine speeds.

The data are presented in figures 11 to 13. Each figure shows both brake specific fuel consumption and brake power. Figures 11 and 12 present engine performance as a function of engine speed and stroke at mean compression-space pressures of 3 and 5 MPa. Figure 13 shows engine performance as a function of engine speed and mean compression-space pressure for an engine stroke of 20 mm; this was the only stroke run at a pressure of 7 MPa. The range of testing included mean compression-space pressures of 3 to 7 MPa, engine strokes of 20 to 40 mm, and engine speeds of 1500 to 3500 rpm.

The brake power increases with increasing engine stroke for all combinations of speed and pressure. A power curve fit (brake power = constant times the stroke raised to an exponent) on the engine test data shows that, for a

given engine speed and mean compression-space pressure, the brake power varies with the stroke raised to a power of 2 to 2.2. The NASA Lewis Stirling engine computer simulation has been modified to simulate the Advenco engine. A similar analysis on the computer simulation predictions indicated an exponent of 1.8 to 1.9. The NASA Lewis Stirling engine computer simulation is described in reference 5.

For a given pressure level, the engine efficiency continuously increases (lower brake specific fuel consumption) with increasing stroke at the lower speeds. However, at the higher engine speeds an intermediate value of stroke gives the highest efficiency (figs. 11 and 12). Predictions by the Lewis Stirling engine computer simulation also exhibit this behavior. This is apparently related to the engine design for maximum efficiency at part power.

The maximum brake power recorded was 4.60 kW at a 5-MPa mean compression-space pressure, 2500-rpm engine speed, and 34-mm engine stroke. The maximum efficiency was 447 g/kW-hr at a 5-MPa pressure, 2000-rpm speed, and 34-mm stroke. This maximum efficiency corresponds to a brake gross thermal efficiency of about 16.9 percent.

Considering all engine testing to date, the maximum power and efficiency obtained were 5.10 kW and 393 g/kW-hr. This brake specific fuel consumption corresponds to a brake gross thermal efficiency of 19.3 percent. These power and efficiency values were recorded for a run at a 5-MPa mean compression-space pressure, 2000-rpm engine speed, 35-mm engine stroke, 625 °C heater-tube gas temperature, and 32 °C cooling-water inlet temperature. The brake gross thermal efficiency is defined as the brake power divided by the heat in from the fuel. The heat in from the fuel was calculated using the lower heating value of the fuel.

Figure 14 shows a comparison of engine test data and computer simulation predictions for brake power as a function of engine speed and stroke. The curves are for a mean compression-space pressure of 5 MPa. Note that the difference between the predictions and the test data increases primarily with engine speed. As described previously, the computer simulation predicts changes in brake power with stroke (for constant mean pressure and speed) reasonably well. The same is true for brake power as a function of mean pressure. Thus, the differences obtained between engine test data and computer simulation predictions appear to be caused mainly by speed-related effects. These could include underestimated mechanical losses in the drive system (as indicated by the drive system failure discussed in the next section) or an underprediction of flow losses in the heat exchangers. Further code validation efforts will be made to investigate these differences.

Drive System Failure

The test data were taken by starting at the lower values of mean compression-space pressure and engine stroke and then progressively increasing these parameters. While continuing this upward progression of pressure and stroke, a major drive system failure occurred. The engine test conditions at the time of the failure were a 5-MPa mean compression-space pressure, 40-mm engine stroke, and 3000-rpm engine speed. A data point at 3500 rpm and this same pressure and stroke had been completed just before this point.

The failure began when one of the crossheads began binding in its bore in the rear crankcase. The crossheads are made of high-strength aluminum with steel sleeves shrink-fitted over the endpieces. As the friction increased, the steel sleeve seized in the bore and was pulled off the crosshead. The consequent deflection of the crosshead caused one of the sliders to be squeezed out of its retainer cup. The other slider then became free of its retainer cup as the load on the crosshead was relieved. These sliders, loose in the drive system, scratched and gouged various parts, particularly the swash-plate surface (fig. 15) and the rear surface of the front crankcase.

The unbalanced load caused by the loss of one crosshead resulted in an overload on the thrust bearing. When the bearing support failed, the main shaft moved rearward. The movement broke the rear crankcase (fig. 16) at its connection to the front crankcase section and also broke the chain on the oil pump drive.

Examination of figure 16 shows the crosshead sleeve stuck in its bore, the initial event of this failure. The photograph of the damaged front crankcase and several of the crossheads and sliders (fig. 17) shows the dented retainer cup from which the first slider escaped on the crosshead farthest to the left. The broken lip of the thrust bearing support can also be seen.

Originally, the failure was thought to be primarily due to inadequate lubrication of the crosshead in its bore. The original design made no specific provision for bringing oil directly to the crosshead-bore interface. Crankcase oil was splashed indirectly on the crosshead when it was out of its bore and then drawn into the bore as the crosshead moved in. However, the rollsock seal requires a tight clearance between the crosshead and its bore. This tight clearance and the sharp-edged entrance to the bore minimized the amount of oil taken in. Both the front and rear crankcase bores were lubricated in this manner.

After the failure spare front and rear crankcase sections were chosen from an inventory of spare parts for the engine rebuild. On dimensional inspection a large misalignment was found between the respective bores of the two crankcase sections. This misalignment was probably present in the crankcases used in the failed engine and could have greatly increased the forces acting on the crossheads. We now believe that both this misalignment and the lack of adequate lubrication were the main reasons for the drive system failure.

The engine is being rebuilt with corrections for these problems:

(1) After detailed inspection procedures the crosshead bores of the rear crankcase were increased by about 0.50 mm. This allows the best possible alignment between the centers of the bores of the front and rear crankcases.

(2) The two crankcases are castings made of 390 aluminum-silicon alloy. The crosshead bores were honed with special procedures to ensure a silicon running surface in the bore.

(3) Spare crossheads were modified to fit the new crankcase dimensions. Rather than being sleeved, they were coated with silver as their primary surface with a flashing of tin for fricton and wear characteristics. Their edges were rounded to minimize oil removal as the crosshead enters the bore.

(4) Pressurized lubrication was provided to the crosshead bores of the rear crankcase by installing direct feeds to the rear of these bores.

(5) Thermocouples were added in the walls of the crosshead bores of the rear crankcase as a possible aid in detecting problems before catastrophic failure.

Comparison of Part-Load Efficiencies by Varying Stroke and by Varying Pressure

The Lewis Stirling-engine computer simulation was used to compare steady-state performance at part loads achieved by varying the stroke at maximum pressure (variable-stroke control) and by varying the pressure at maximum stroke (mean-pressure control). Figure 18 presents these results for hydrogen and helium working fluids. Brake thermal efficiency (defined as the brake output divided by the heat into the engine - does not include burner losses) is shown as a function of engine speed and percent of maximum brake power. The maximum brake powers for both hydrogen and helium were obtained at the maximum stroke of 48.5 mm, the maximum mean compression-space pressure of 10 MPa, and an engine speed of 4000 rpm. For hydrogen, the maximum output was 43.2 kW, and for helium, 24.2 kW.

Two curves are shown for each speed. The curve for varying stroke was obtained by running several different strokes at the maximum mean compression-space pressure of 10 MPa. The curve for varying pressure was made by running several different pressures at the maximum stroke of 48.5 mm. The temperatures for all curves were 720 °C heater-tube outside wall temperature and 50 °C cooling-water inlet temperature.

Figure 18(a) shows an efficiency improvement for varying stroke for both speeds with hydrogen working fluid. The improvement is largest at the higher speed and increases as the power level decreases. Figure 18(b) shows greater efficiency improvements for varying stroke with helium. The efficiency improvements for varying stroke compared with the varying pressure case at the same power level are due in part to lower flow losses (as predicted by the computer simulation) through the heat exchangers for a given part-load point. Also, heat losses that tend to decrease with reduced stroke and pressure ratio (such as shuttle losses) contribute to this efficiency improvement. For the same control temperatures and power levels, the variable-stroke runs exhibit higher hot-end and lower cold-end gas temperatures than do the varying pressure cases; the engine efficiency increases as the gas temperature ratio increases. These gas temperatures are dependent on the engine hot-end and cold-end heat flows and on the heat-transfer coefficients in the heat exchangers.

The large efficiency improvement shown for the helium cases of figure 18(b) is related in part to the Advenco engine being designed for hydrogen working fluid. Reoptimizing the heat exchangers for helium would decrease the efficiency improvement for varying the stroke. For instance, the helium heat exchangers would probably be shortened to reduce the flow losses.

Because of the drive-system failure, test data have not been taken at the maximum stroke or pressure. However, comparisons of part-load efficiencies were made between the low-power engine test data and the computer simulation

predictions corresponding to these test data. Figure 19 shows the comparison for an engine speed of 2500 rpm. The maximum brake power points for both the test data and the simulation predictions corresponded to a 34-mm engine stroke and 5-MPa mean compression-space pressure. Brake thermal efficiency is plotted as a fraction of the maximum brake thermal efficiency. This was used because the computer simulation overpredicts engine efficiency, due largely to an overprediction of engine power output.

The shapes of the curves are similar for both the computer simulation predictions and the engine test data. The engine test data suggest a somewhat larger efficiency improvement (in percent of maximum efficiency) for varying the stroke compared with varying the pressure than do the computer simulation results. Note, however, that only two test points were taken that could be used to determine the curves for varying the pressure.

CONCLUDING REMARKS

The initial test data and computer simulation predictions indicate a steady-state efficiency improvement at part loads for variable-stroke control compared with mean-pressure control. Following rebuild of the Advenco engine, steady-state testing will be completed with both helium and hydrogen working fluids to quantify the magnitude of this improvement. No problems have been encountered with the Stirling cycle functioning at reduced strokes.

Simplified transient tests will be run to investigate the control-system response. Other expected benefits of variable-stroke control (compared with mean-pressure control), such as reduced control system complexity and reduced working fluid leakage, will be addressed as conditions permit.

The drive system failure demonstrates the need to provide proper alignment and adequate lubrication in the design and fabrication of the crossheads and crankcase bores. The variable-angle swash-plate drive will continue to be evaluated as a means for obtaining variable-stroke control.

REFERENCES

1. Vos, J.: Design Characteristics of an Advanced Stirling Engine Concept. Proceedings of the 14th Intersociety Energy Conversion Engineering Conference, Vol. 1, American Chemical Society, 1979, pp. 1191-1196.

2. Kitzner, Ernest W.: Automotive Stirling Engine Development Program. DOE/NASA/4396-4, NASA CR-159836, 1980.

3. Meijer, R.J.; and Ziph, B.: Variable Stroke Power Control for Stirling Engines. SAE Paper 810088, 1981.

4. Miller, Robert L.: Escort: A Data Acquisition and Display System to Support Research Testing. NASA TM-78909, 1978.

5. Tew, Roy C., Jr.: Computer Program for Stirling Engine Performance Calculations. DOE/NASA/51040-42, NASA TM-82960, 1983.

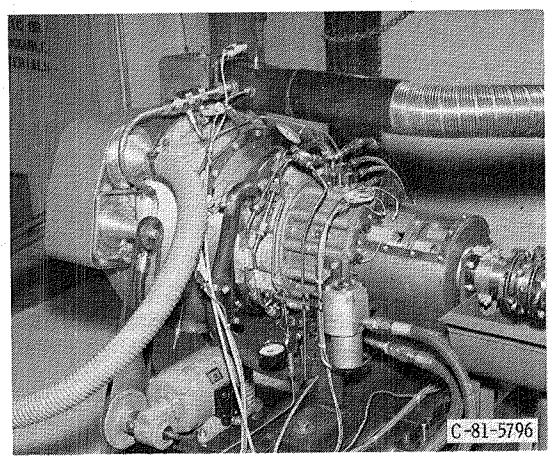

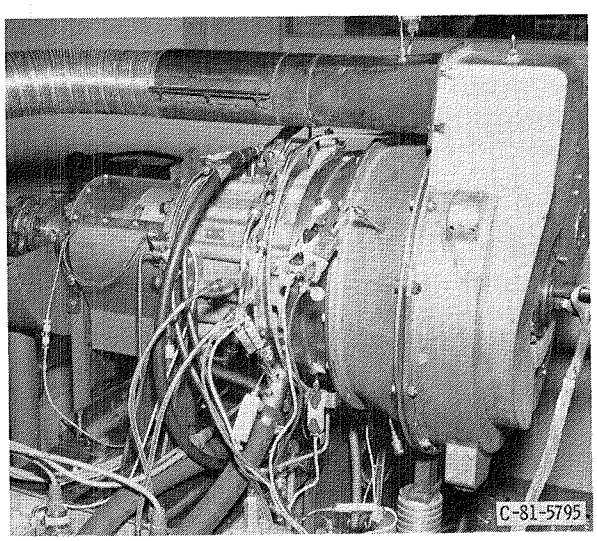

Figure 1. - Advenco Stirling engine.

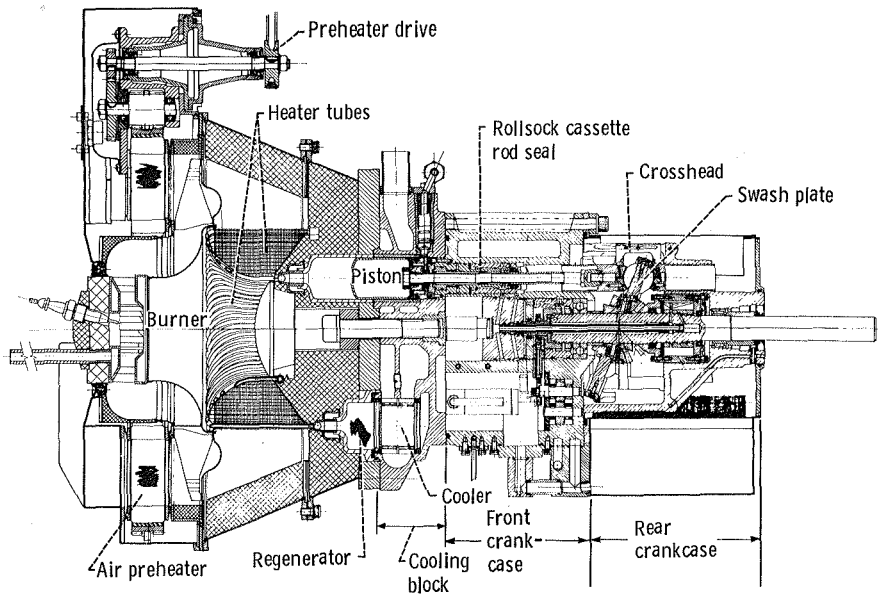

Figure 2. - Advenco Stirling engine cross-section.

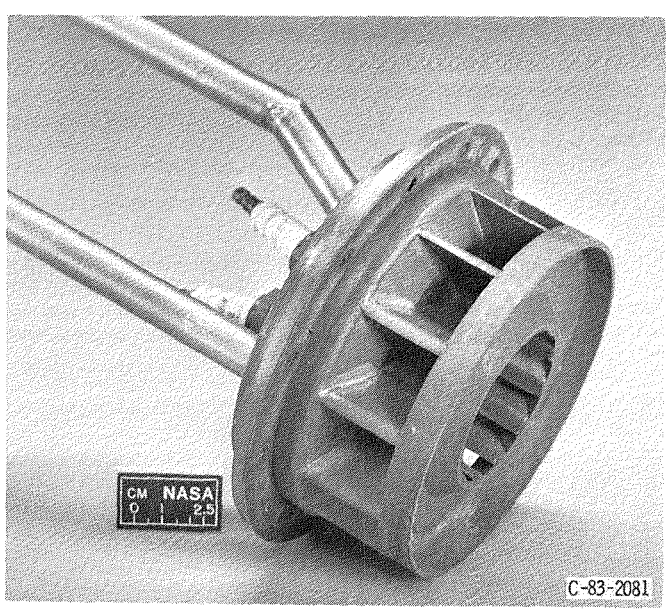

Figure 3. - Vortex gas burner.

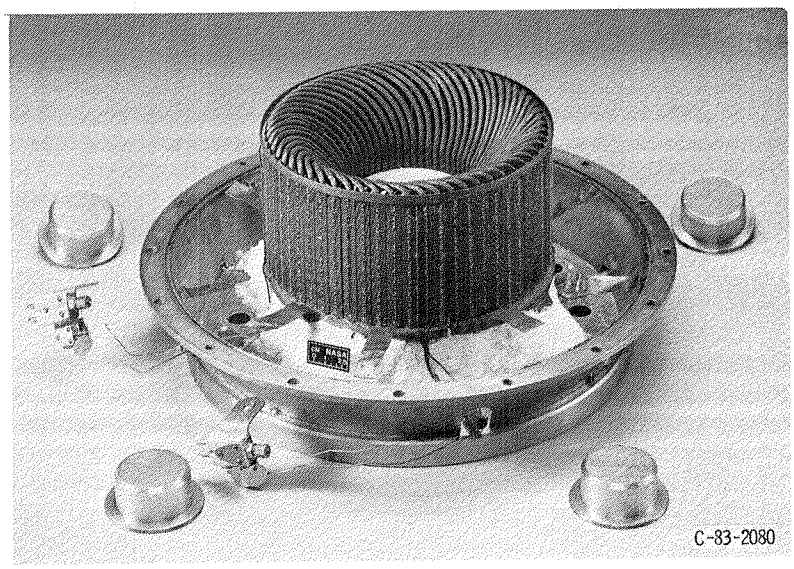

Figure 4. - Heater head with regenerators.

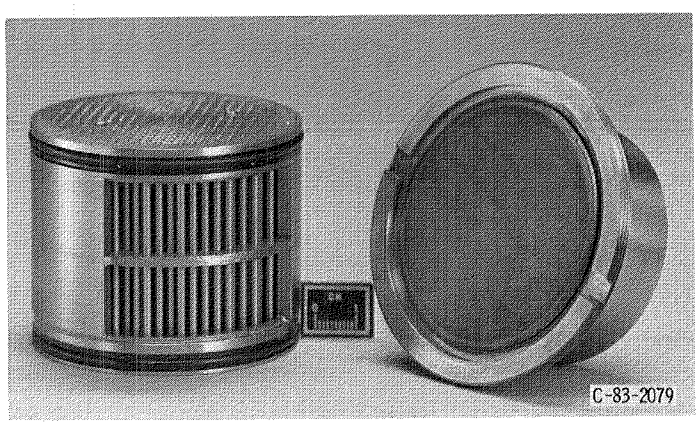

Figure 5. - Cooler and regenerator.

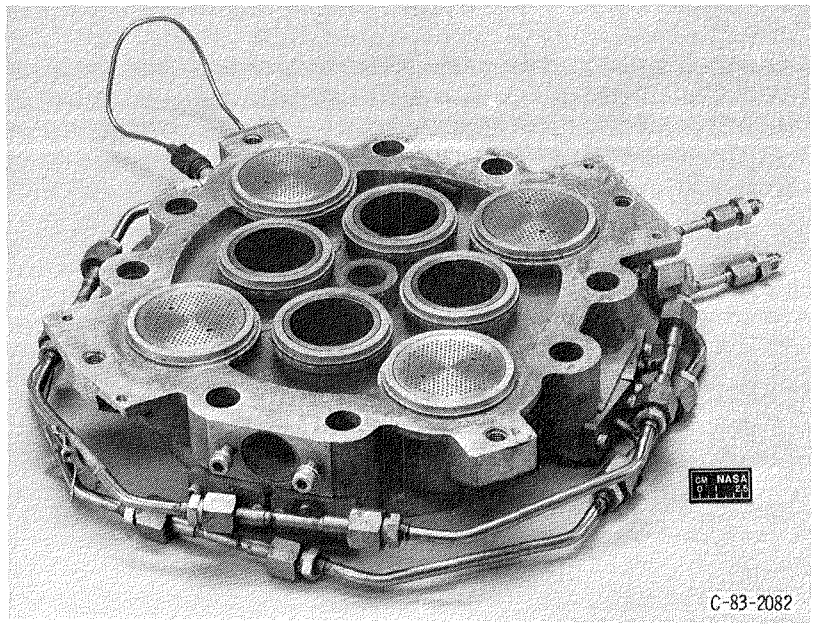

Figure 6. - Cooling block with coolers installed.

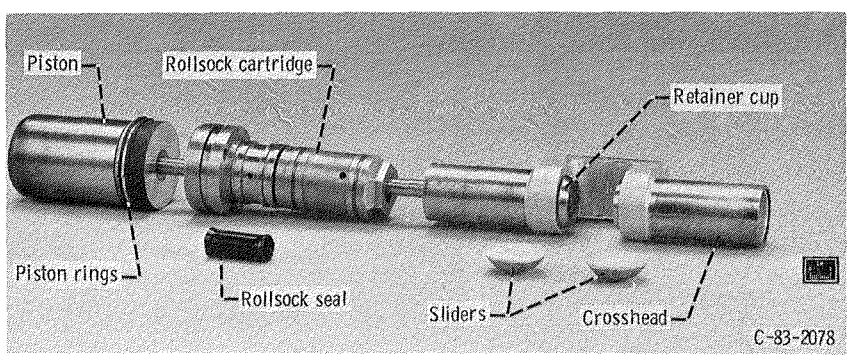

Figure 7. - Piston, rollsock cartridge and seal, and crosshead with sliders.

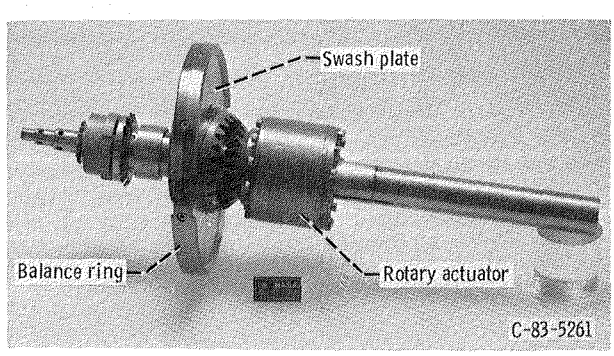

Figure 8. - Variable-angle swash-plate assembly.

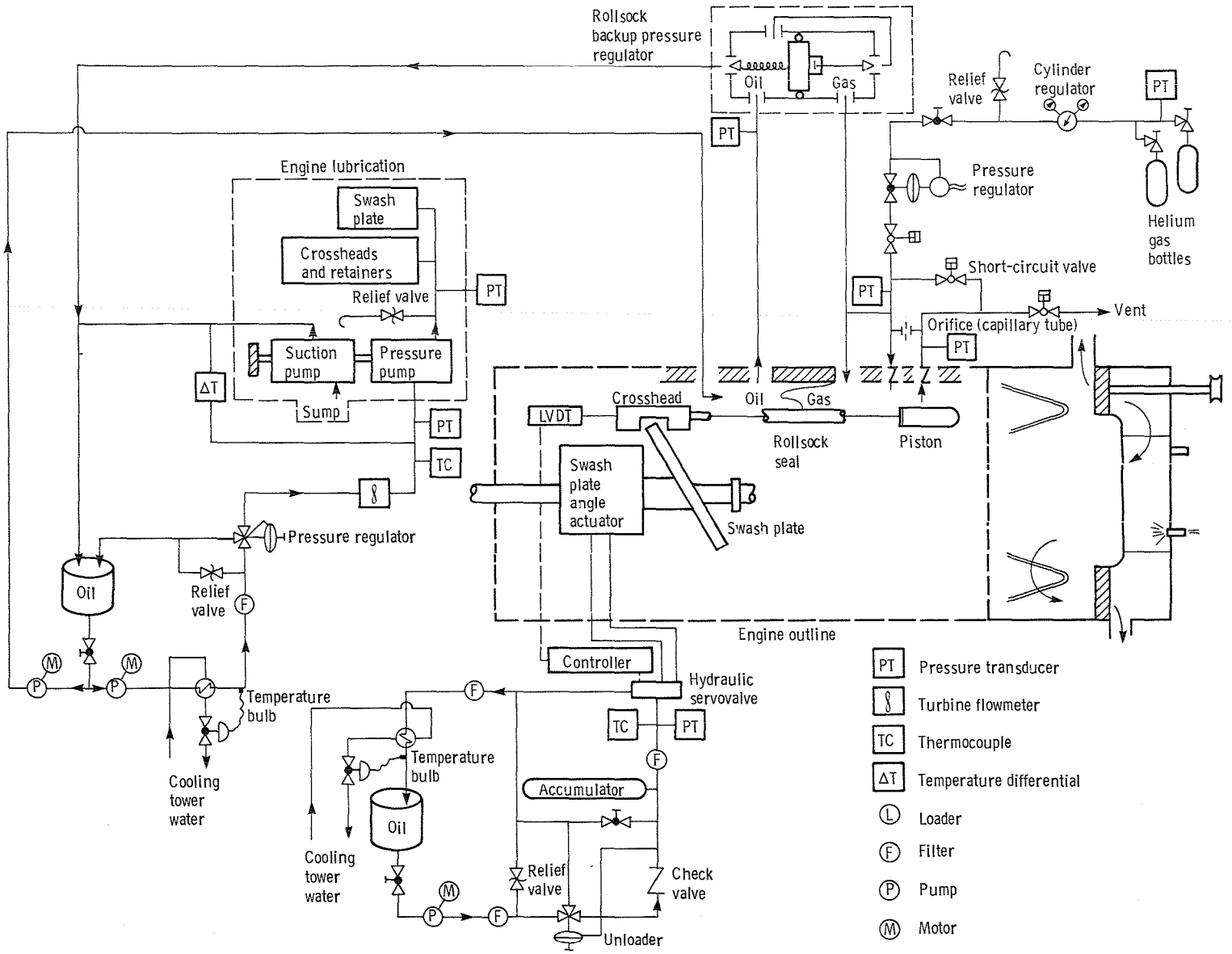

Figure 9. - Advenco test schematic of oil systems and helium pressurization system.

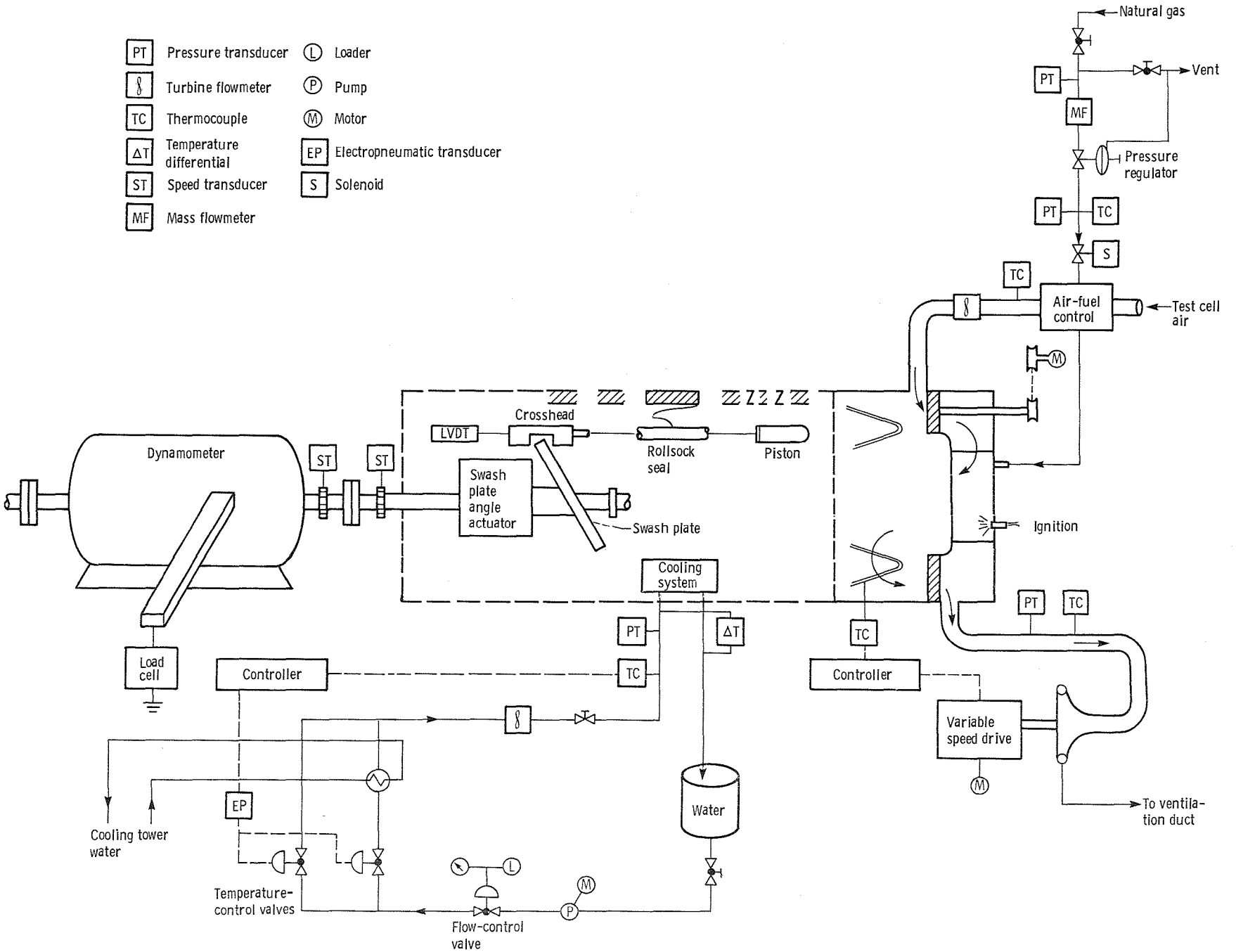

Figure 10. - Advenco test schematic of cooling-water system, air-fuel system, and engine load.

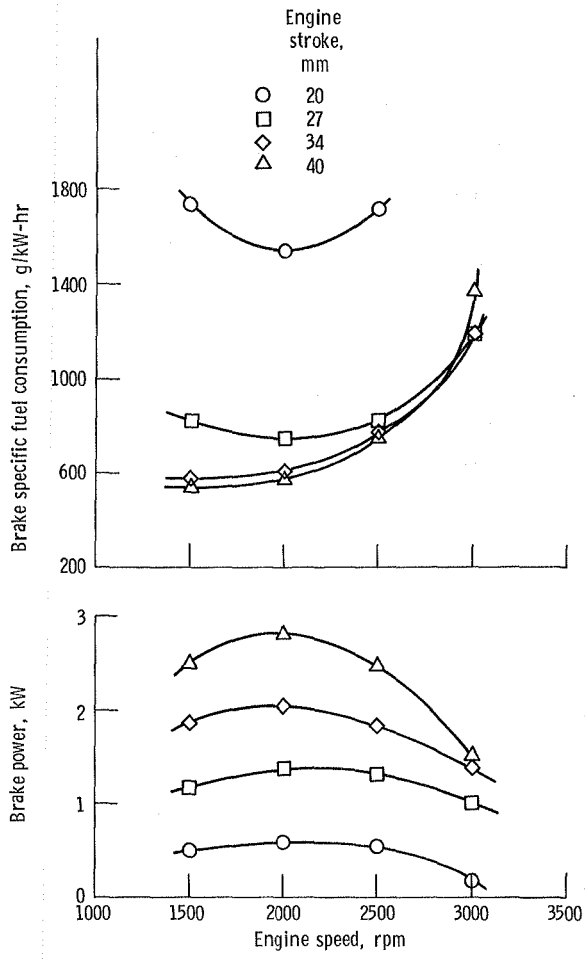

Figure 11. - Engine performance as function of engine speed and engine stroke for mean compression-space pressure of 3 MPa. Heater-tube gas temperature, 625 °C; cooling-water inlet temperature, 50 °C; helium working fluid.

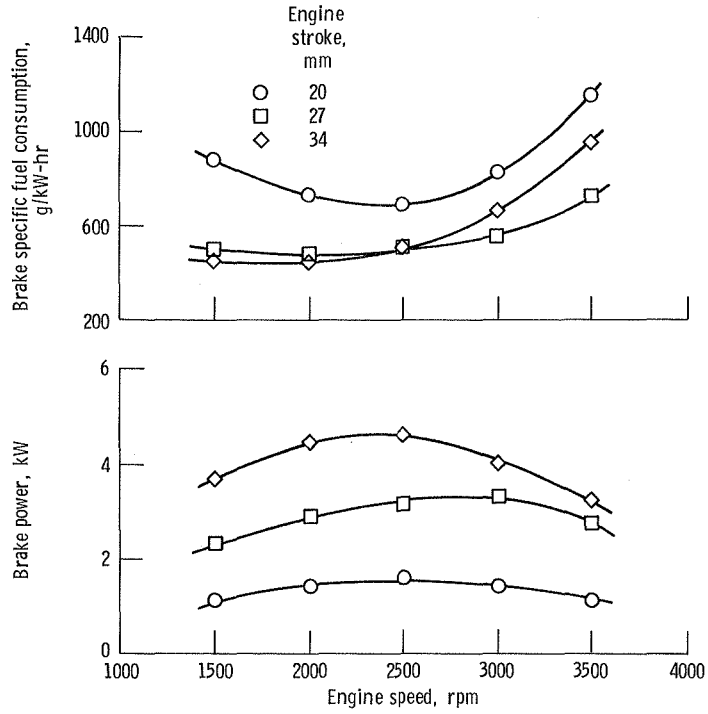

Figure 12. - Engine performance as function of engine speed and engine stroke for mean compression-space pressure of 5 MPa. Heater-tube gas temperature, 625 °C; cooling-water inlet temperature, 50 °C; helium working fluid.

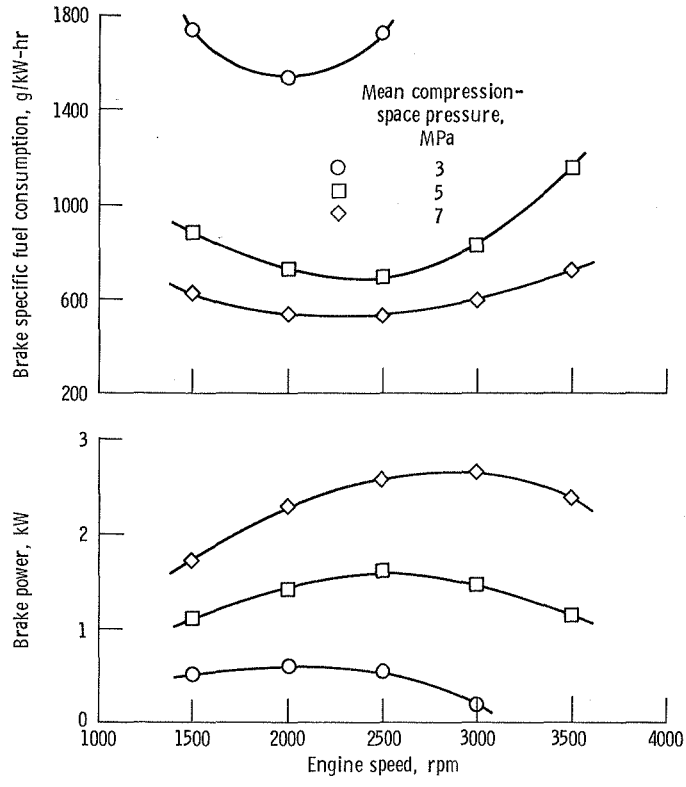

Figure 13. - Engine performance as function of engine speed and mean compression-space pressure for an engine stroke of 20 mm. Heater-tube gas temperature, 625 °C; cooling-water inlet temperature, 50 °C; helium working fluid.

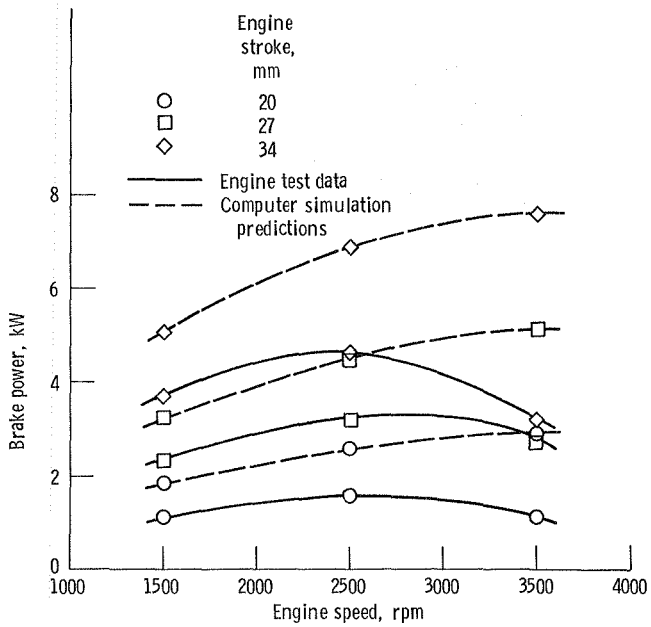

Figure 14. - Comparison of engine test data and computer simulation predictions for brake power as a function of engine speed and engine stroke. Mean compression-space pressure, 5 MPa. Heater-tube gas temperature, 625 °C; cooling-water inlet temperature, 50 °C; helium working fluid.

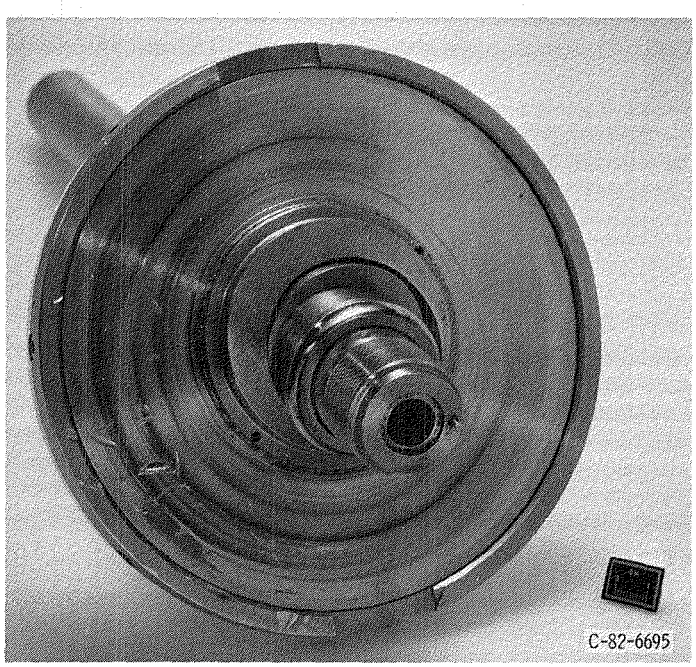

Figure 15. - Damaged swash plate from drive system failure.

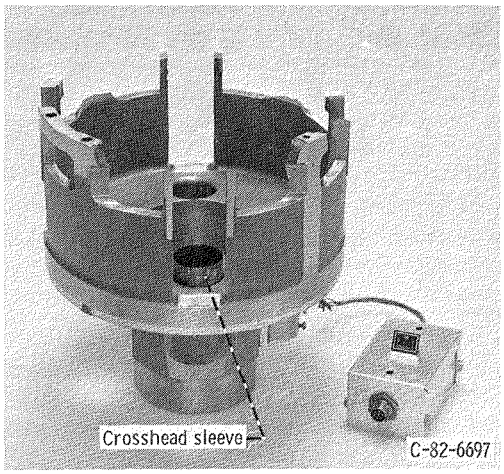

Figure 16. - Damaged rear crankcase from drive system failure; note the crosshead sleeve stuck in bore.

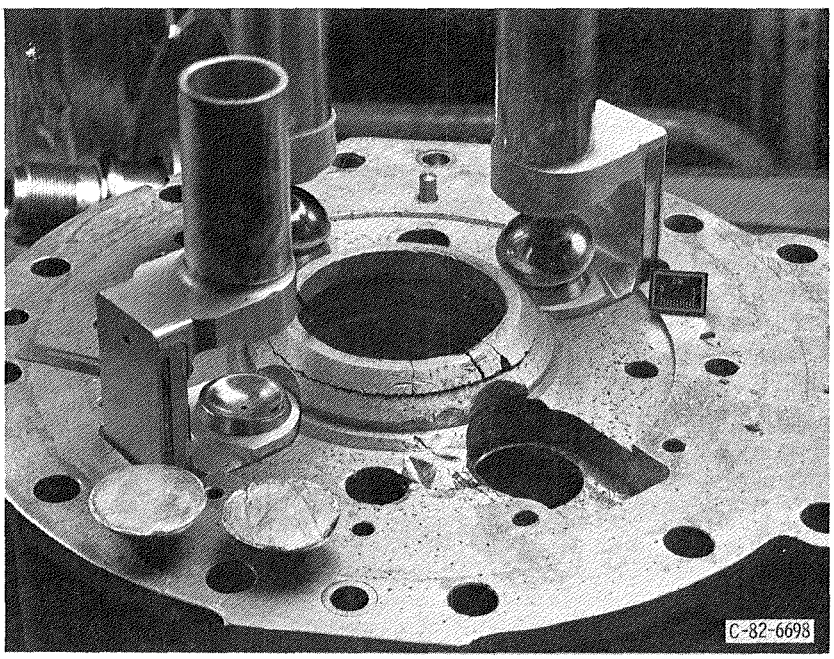

Figure 17. - Damaged front crankcase, crossheads, and sliders from drive system failure.

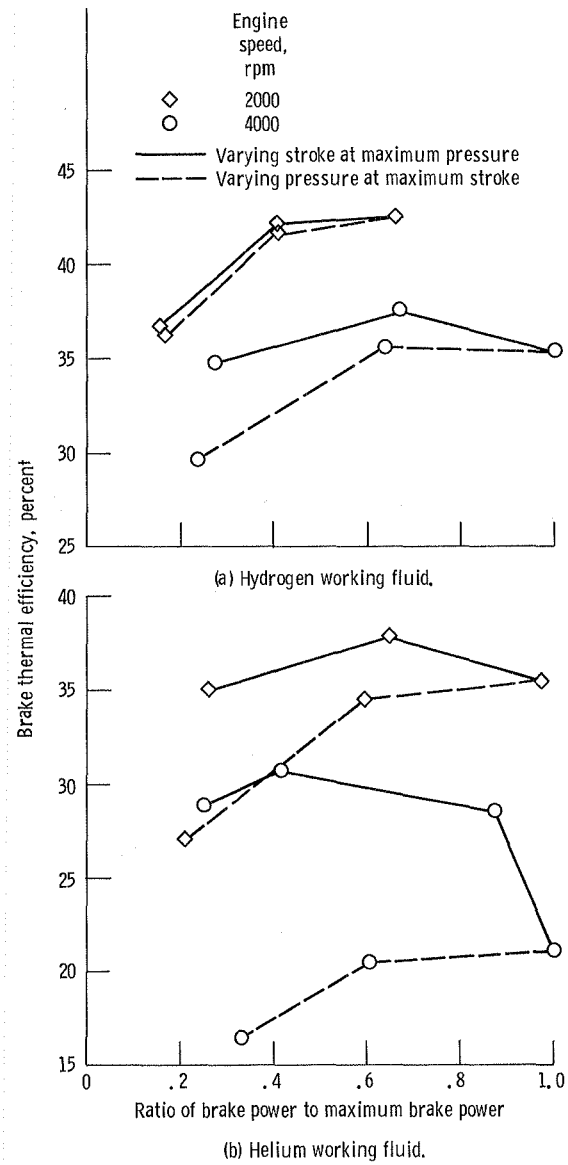

Figure 18. - Comparison of computer simulation predictions of part-load efficiencies.

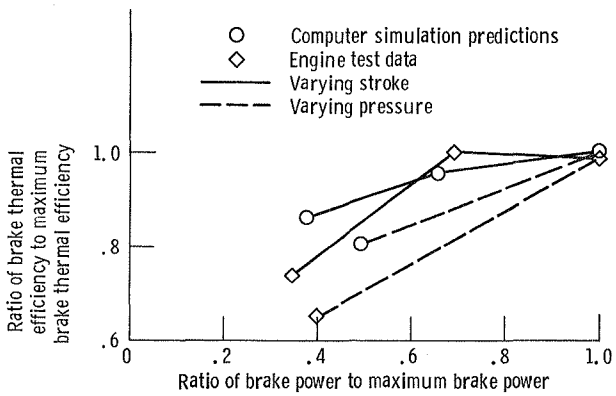

Figure 19. - Comparison of engine test data and computer simulation predictions for obtaining part-load efficiencies. Helium working fluid; engine speed, 2500 rpm. Maximum brake powers: 4.6 kW for engine test data and 6.9 kW for simulation predictions. Maximum brake thermal efficiencies: 16.4 percent for engine test data and 30.8 percent for simulation predictions.

1. Report No.	2. Government Accession No.	3. Recipient's Catalog No.
NASA TM-86875		

4. Title and Subtitle	5. Report Date
Initial Testing of a Variable-Stroke Stirling Engine	February 1985
	6. Performing Organization Code 778-35-03
7. Author(s) Lanny G. Thieme	8. Performing Organization Report No. E-2336
	10. Work Unit No.
9. Performing Organization Name and Address National Aeronautics and Space Administration Lewis Research Center Cleveland, Ohio 44135	11. Contract or Grant No.
	13. Type of Report and Period Covered Technical Memorandum
12. Sponsoring Agency Name and Address U.S. Department of Energy Office of Vehicle and Engine R&D Washington, D.C. 20546	14. Sponsoring Agency Code Report No. DOE/NASA/51040-58

15. Supplementary Notes

Final report. Prepared under Interagency Agreement DE-AI01-77CS51040. Shorter version published in Proceedings of the Twenty-first Automotive Technology Development Contractors' Coordination Meeting, Dearborn, Michigan, November 14-17, 1983.

16. Abstract

In support of the U.S. Department of Energy's Stirling Engine Highway Vehicle Systems Program, NASA Lewis Research Center is evaluating variable-stroke control for Stirling engines. The engine being tested is the Advenco Stirling engine; this engine was manufactured by Philips Research Laboratories of the Netherlands and uses a variable-angle swash-plate drive to achieve variable stroke operation. This report describes the engine, presents initial steady-state test data taken at Lewis, and describes a major drive system failure and subsequent modifications. Computer simulation results are presented to show potential part-load efficiency gains with variable-stroke control.

17. Key Words (Suggested by Author(s))	18. Distribution Statement
Stirling engine; Stirling cycle; Heat engine; Variable stroke; Swash plate	Unclassified - unlimited STAR Category 85 DOE Category UC-96

19. Security Classif. (of this report)	20. Security Classif. (of this page)	21. No. of pages	22. Price*
Unclassified	Unclassified		A02

*For sale by the National Technical Information Service, Springfield, Virginia 22161

End of Document